

Investigation of the Mathieu Instability of Roll Motion by a Time-Domain Viscous-Fluid Method

S.-W. Liao and R. W. Yeung

Mechanical Engineering & Ocean Engineering

University of California at Berkeley, Berkeley, California 94720-1740, USA

Introduction

Correct predictions of response of floating bodies in waves have been of great interest in the field of naval architecture and ocean engineering. Time-domain analysis based on potential-flow theory remains a popular approach (see e.g., Vinje and Brevig, 1980, Tanizawa and Naito, 1997, Van Daalen 1993, Wu & Eatock-Taylor, 1996, Celebi & Beck, 1997), even though in many occasions viscous effects cannot be ignored.

Roll response near its resonance condition, in particular, is strongly affected by viscous damping, not only in terms of the steady-state response amplitude, but also in terms of the stability or boundedness of the response itself, as we will address in this paper. It is possible to account for viscous effects but introducing damping in an empirical way (see, e.g., Himeno, 1981, Cointe et al., 1990, Sen, 1993). Nonetheless, it would be highly desirable to remove such empiricism by including the consideration of viscosity at the outset of the flow problem. This has been successfully pursued by Yeung and Liao (1999) in their FSRVM (Free-Surface Random-Vortex Method) method. In this paper, we explore the analysis and the computational basis of how the coupled multiple-degrees of freedom response of a floating body can critically depend on the presence of viscous damping.

The interesting phenomenon of Mathieu instability, arisen from the coupling between heave and roll motion (Paulling and Rosenberg, 1959) is investigated. The effects associated with the presence of bilge keels and fluid viscosity on the response near a “troublesome” resonant condition are addressed. The nonlinear coupling between heave and roll is vital, thus the issue is very much related to large-amplitude motion. A cylinder having interesting geometrical properties is devised for both experiments and computations. This cylinder is shown to be dynamically unstable under certain conditions according to the Mathieu equation.

Nonlinear heave-roll coupling

It was known from the time of Froude (1863) that the coupling between heave and roll can result in unstable ship motion. The phenomenon was investigated experimentally and theoretically by Paulling and Rosenberg (1959) for a ship undergoing forced oscillation in heave with an initial roll angle. The instability is related to the geometrical properties of a ship, the location of center of gravity, and the amplitude of the heave motion. This instability in roll is most likely to occur at the heave resonance frequency ω_y when the heave amplitude is sufficiently large.

Based on the equilibrium between inertia and restoring moment, the roll equation of a cylinder about its center of gravity (Paulling and Rosenberg, 1959) can be written as

$$(I_g + \mu_{33}) \frac{d^2 \alpha}{dt^2} + M_b g \overline{GM} \alpha + K_{\alpha y} \alpha y_o \cos(\omega_y t) = 0, \quad (1)$$

where I_g is the moment of inertia, μ_{33} the added moment of in-

ertia, M_b the mass, \overline{GM} the metacentric height, α the roll displacement, y the heave displacement, and y_o the amplitude of heave displacement (see Fig. 1). The last term of the equation, $K_{\alpha y}$, is the nonlinear restoring moment per unit roll and unit heave displacements. The nonlinear coefficient $K_{\alpha y}$ was given in terms of body geometry by Paulling and Rosenberg (1959). However, for a wall-sided cylinder, it is not difficult to show that $K_{\alpha y} = \rho g \overline{OG} A_w$, where \overline{OG} is the distance between the center of gravity and the body center and $A_w = B$ being the (two-dimensional) waterplane area for the cylinder. Equation (1) can be nondimensionalized to obtain the standard Mathieu equation (see for example, Jordan and Smith, 1988):

$$\frac{d^2 \alpha}{d\tau^2} + (\delta + \epsilon \cos \tau) \alpha = 0, \quad (2)$$

$$\delta \equiv (\omega_\alpha / \omega_y)^2, \quad \epsilon \equiv \delta (y_o / \overline{GM}) (K_{\alpha y} / M_b), \quad (3)$$

and $\tau = \omega_y t$. The heave and roll natural frequencies are defined as

$$\omega_y = (\rho g B / (M_b + \mu_{22}))^{1/2}, \quad (4)$$

$$\omega_\alpha = (M_b g \overline{GM} / (I_g + \mu_{33}))^{1/2}. \quad (5)$$

Equation (2) is known to be unstable at $\delta \approx 1/4$ even for a small value of ϵ , the nonlinear coupling term. This is equivalent to saying that the cylinder is unstable when $\omega_\alpha / \omega_y = 1/2$ even with only a small amount of forcing from heave. The stable and unstable regions were obtained by Stoker (1950) using perturbation methods. This is plotted in Fig. 2, which identifies that the Mathieu equation is highly unstable around $\delta = 1/4$. Beyond this critical value of δ , a finite amount of heave forcing is needed to induce roll instability.

In the figure, additional stable regions due to the presence of a linear damping term is also plotted. The damped Mathieu equation with linear coefficient μ , is given by:

$$\frac{d^2 \alpha}{d\tau^2} + \mu \frac{d\alpha}{d\tau} + (\delta + \epsilon \cos \tau) \alpha = 0, \quad (6)$$

$$\mu \equiv \frac{\lambda_{33}}{\omega_y (I_g + \mu_{33})}. \quad (7)$$

The source of damping can result from both wave generation and viscous dissipation associated with the motion. The stability of Eqn. (6) is well studied especially for $\delta \approx 1/4$ (e.g., see Jordan and Smith, 1988). The Mathieu equation with damping is stable if the index

$$c_1 \equiv \left[\left(\delta - \frac{1}{4} \right)^2 - \frac{1}{4} (\epsilon^2 - \mu^2) \right] > 0. \quad (8)$$

This means for $\delta = 1/4$ Eqn. (6) is unstable whenever $\epsilon > \mu$. Physically, this implies that a critical amount of damping is needed for a given heave response in order to suppress the instability. Investigation of this instability condition in the context of a cylinder in waves is therefore of fundamental and practical interest.

A “marginally stable” cylinder

In our laboratory tests and computer modeling, a marginally (dynamically) stable rectangular cylinder is designed so that its δ value is slightly larger than $1/4$. The unstable condition of Eqn. (8) can be acquired presumably by introducing bilge keels. The argument would be that the bilge keel would increase the added inertia μ_{33} , resulting in a δ very much closer to $1/4$. Thus the cylinder would easily fall into the unstable region of Fig. 2. All of these expectations are based on a damping estimate using inviscid theory alone. In physical reality, while the δ value moves closer to the critical value of $1/4$ because of the bilge keels, the viscous damping or its “linear equivalent” value will increase also. As a matter of fact, the damping would increase sufficiently that the cylinder could remain in the stable region. The laboratory experiments of Roddier et al (2000) indicate that the cylinder has no roll stability problem with or without bilge keels. This subtle behavior offers a challenging test for a time-domain computational model such as FSRVM, which can have viscosity turned on or off.

The geometrical properties of the cylinder are: beam to draft ratio $B/H = 2$, corner radius of bilges $R = 0.0205B$, center of gravity $y_g = -0.141B$, and the radius of gyration $R_g = 0.352B$. The depth of the bilge keels is 6% of the beam B . Details of the keels may be found in Roddier et al. (2000.) To calculate the resonant frequencies, ω_y and ω_α , the “FSRVM” of Yeung and Vaidhyanathan (1994) is applied to simulate *forced* heave and roll oscillations to obtain added mass and added moment of inertia coefficients. After μ_{22} and μ_{33} are obtained for both inviscid and viscous solutions over a range of frequency (Yeung et al., 1998), ω_y and ω_α are calculated through iteration using Eqns. (4) and (5). The damping or equivalent linear damping coefficients λ_{33} are also obtained through the simulations of forced oscillations.

The stability investigation is performed at an incident-wave frequency of $\tilde{\omega} \equiv \omega \sqrt{B/2g} = 0.7455$, and wave amplitude to wavelength ratio $A/\lambda = 2\%$. This frequency is very close to the resonant heave frequency of the model. There are four configurations of the cylinders considered in this study: inviscid and viscous fluid simulations for the cylinder, each for the case of with, or without bilge keels. Table 1 summarizes the estimated parameters in Eqn. (6) for these four scenarios based on frequency domain solutions. Case *I1* & *I2* represent inviscid fluid modeling, whereas Case *V1* & *V2* represent full Navier Stokes solutions of the problem. In the case of viscous flow, the equivalent linear damping coefficient μ is obtained by Fourier analysis of the time history of the applied moment.

In Table 1, the stability index c_1 of Eqn. (8) is also shown for the specific values of δ , ϵ , and μ . Thus, the cylinder is stable if $c_1 > 0$ and vice versa. It is seen that Case *I2*, an inviscid model with bilge keels, will have an unstable roll response, while the other cases are dynamically stable.

The boundaries of stability in Fig. 2 near $\delta = 1/4$ can be obtained by setting Eqn. (8) equal to 0. Figure 3 shows the “maximum” heave-motion parameter ϵ for stability as a function of δ . In each curve μ is taken as the minimum damping based on the specific ϵ and δ values for the case at issue. This plot shows that Case *I2* is clearly unstable while Case *V2* has the largest amount of stability margin.

Time-domain theoretical model

The computational model FSRVM used to obtain the motion of a freely-floating body in a viscous fluid is fully nonlinear. The boundary-value problem is defined in Figure 4, where a vorticity and stream-function formulation is used. The computational domain is bounded by the body ∂D_b , the free surface ∂D_f , and the

open boundary ∂D_Σ . On the free surface, an oscillating pressure patch is used to generate waves. The vorticity equation is solved by a fractional-step of successive convection and diffusion. The convection calculations are carried out using a complex-variable integral-equation formulation. The details can be found in Yeung and Liao (1999) and Roddier et al. (2000). Applications of FSRVM to a fixed submerged body in large waves were considered in Yeung et al. (1999).

Since the body is freely floating, the boundary conditions on the body are coupled to the rigid-body dynamics equations. A methodology is established to couple the body accelerations to the boundary conditions of the fluid by using Newton’s Second Law. The following linear system can be derived and solved explicitly for $(\ddot{x}_b, \ddot{y}_b, \ddot{\alpha})$ at any t .

$$\begin{bmatrix} (M_b + A_{11}) & A_{12} & (A_{13} - M_b y_{og}) \\ A_{21} & (M_b + A_{22}) & (A_{23} + M_b x_{og}) \\ (A_{31} - M_b y_{og}) & (A_{32} + M_b x_{og}) & (I_o + A_{33}) \end{bmatrix} \begin{bmatrix} \ddot{x}_b \\ \ddot{y}_b \\ \ddot{\alpha} \end{bmatrix} = \begin{bmatrix} W_{41} + M_b x_{og} \dot{\alpha}^2 \\ W_{42} + M_b y_{og} \dot{\alpha}^2 - M_b g \\ W_{43} - M_b g x_{og} \end{bmatrix}. \quad (9)$$

In Eqn. (9), $A_{ij}s$ depend only on the contour of ∂D . On the other hand, $W_{4i}s$ depend on solutions to the fluid velocity and vorticity field, which includes effects of wave excitation and hydrostatic terms.

Numerical results

To establish the validity of the computational model, results given in Roddier et al. (2000) are shown for assessment. Figure 5 shows a comparison between the calculated and measured free-surface elevation for a slightly different frequency, $\omega \approx 0.6$. The results of 3 dof of motion response are shown in Fig. 6. Figures 5 and 6 show that the agreement is very good between calculated and measured results. In the experiments, the model slides unrestrained along a pair of horizontal guides. The friction of these guides need to be accounted for (see Case (c)).

If a cylinder is unstable, a valid numerical model should be able to capture the expected instability. Results of numerical simulations using the FSRVM model are presented for the four configurations discussed in the previous section (see Table 1). Since the instability is associated with excessive heave motion, the instability should disappear if the cylinder is restrained in heave. To verify this, inviscid results are also presented for the cylinder being restrained in heave and sway.

Figure 7 shows the roll displacements of the freely floating cylinder for the same four configurations mentioned. It can be seen that the response is bounded for all cases except for the inviscid case with keels (Case *I2*). This confirms that the time-domain modeling of FSRVM can predict the instability correctly. The roll response for the unstable case shows that the cylinder primarily rolls at the wave frequency for $\tilde{t} < 10$. For $\tilde{t} > 10$, the cylinder starts rolling at the roll natural frequency, which is one half of the wave frequency! Shortly after, the cylinder capsized. Figure 8 shows two sets of inviscid results of roll displacements for the cylinder restrained in heave and sway. The roll response is bounded if there is no heave motion, but grows without bound when there it is restrained from swaying. This also confirms the instability is related to the nonlinear coupling between heave and roll.

Conclusions

The nonlinear effects, associated with bilge keels and fluid viscosity, on the response of cylinders in waves were investigated.

Case		$\tilde{\omega}_y$	$\tilde{\omega}_\alpha$	δ	μ	ϵ	c_1
<i>Inviscid fluid</i>							
I1	No keel	0.7603	0.4194	0.3024	0.1680	0.1719	0.00168
I2	With keels	0.7455	0.3736	0.2511	0.1395	0.1545	-0.00110
<i>Viscous fluid</i>							
V1	No keel	0.7604	0.4131	0.2952	0.1791	0.1633	0.00169
V2	With keels	0.7455	0.3969	0.2834	0.3374	0.1604	0.02361

Table 1: Nondimensional parameters for various numerical cases.

It was shown that the response characteristics were very different depending on whether or not bilge keels and fluid viscosity was considered. For the cylinder with keels, the response showed that the proper modeling of fluid viscosity was critical in order to predict the motion correctly. On the other hand, inviscid-fluid models could predict an instability which is not always present in the physical world.

References

- [1] Cointe, R., Geyer, P., King, B., Molin, B., and Tramoni, M. (1990). *Proc. 18th Symp. on Naval Hydrodyn.*, Ann Arbor, Michigan.
- [2] Froude, W. (1966). *The Papers of William Froude*, INA, 1995. See also *Transactions*, INA, 1863.
- [3] Himeno, Y. (1981). Dept. Naval Arch. & Mar. Engrg., University of Michigan, Rep. no 239.
- [4] Jordan, D. W. and Smith, P. (1988). *Nonlinear Ordinary Differential Equations*, Oxford University Press, Oxford, UK.
- [5] Paulling, J. R. and Rosenberg, R. M. (1959). *J. Ship Res.*, **3**, pp. 36-46.
- [6] Roddier, D., Liao, S.-W., and Yeung, R. W. (2000). *Int'l J. Offshore and Polar Engrg.*, **10**, No 4, pp. 241-248.
- [7] Sen, D. (1993). *J. Ship Res.*, **37**, pp. 307-330.
- [8] Tanizawa, K. and Naito, S. (1997). *Proc. 11th Int'l Offshore and Polar Engrg. Conf.*, Honolulu, Hawaii.
- [9] Van Daalen, E. F. G. (1993). Ph.D. dissertation, University of Twente, The Netherlands.
- [10] Vinje, T. and Brevig, P. (1980). Tech. Rept., The Norwegian Inst. of Tech., Trondheim.
- [11] Wu, G. X. and Eatock-Taylor, R. (1996). *Proc. 11th Int'l Workshop on Water Waves and Floating Bodies*, Hamburg, German.
- [12] Yeung, R. W. and Liao S.-W. (1999). *Proc. 9th Int'l Offshore and Polar Engrg. Conf.*, Brest, France.
- [13] Yeung, R. W., Liao S.-W., and Roddier D. (1999). *Proc. 14th Int'l Workshop on Water Waves and Floating Bodies*, Port Huron, MI.
- [14] Yeung, R. W. and Vaidhyanathan, M. (1994). *Proc. Int'l Conf. on Hydrodyn.*, Wuxi, China.

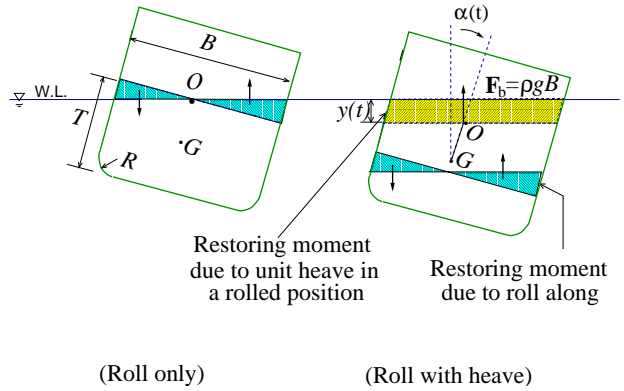


Figure 1: Roll restoring moment with and without heave displacement.

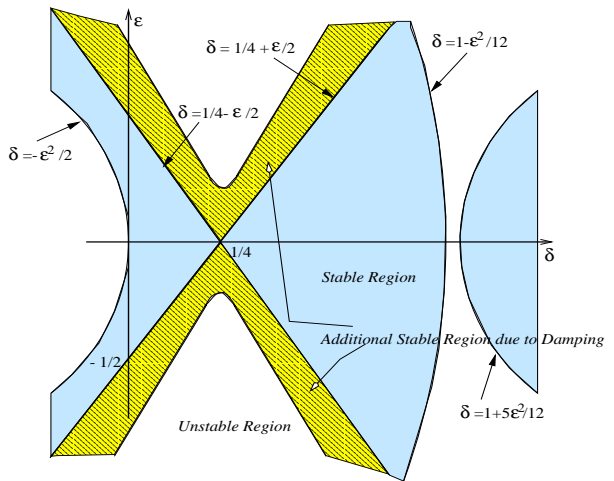


Figure 2: Stoker's approximation of stable and unstable regions for the Mathieu equation.

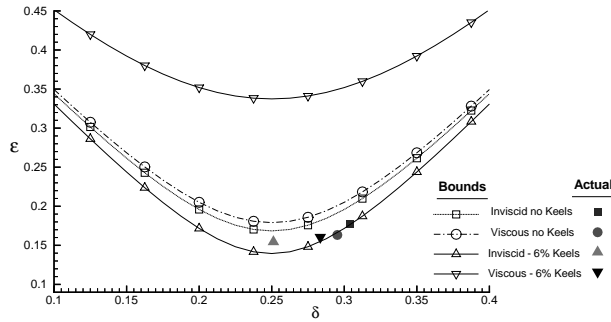


Figure 3: Values and upper bounds for ϵ (for stability) vs. δ .

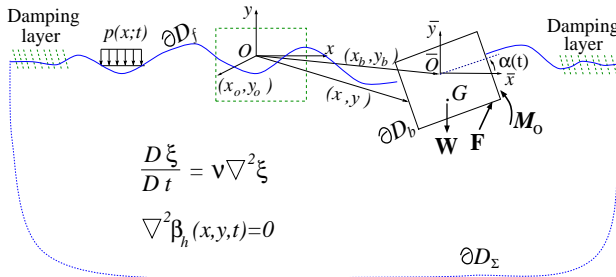


Figure 4: Definitions and the computational domain D .

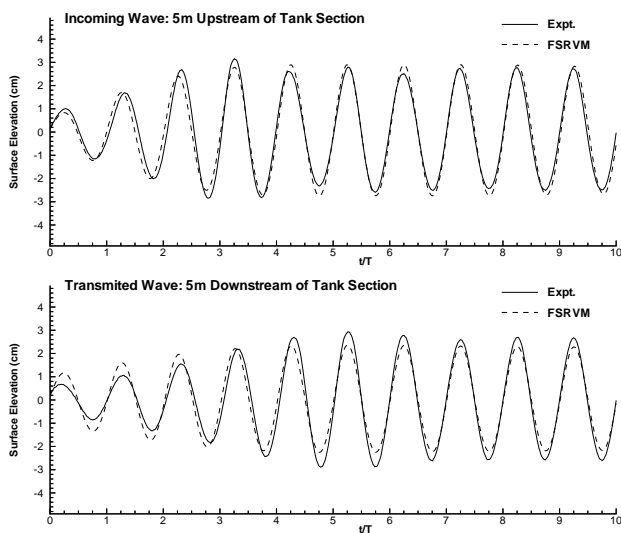


Figure 5: Incident and transmitted waves for $\tilde{\omega} = 0.6$

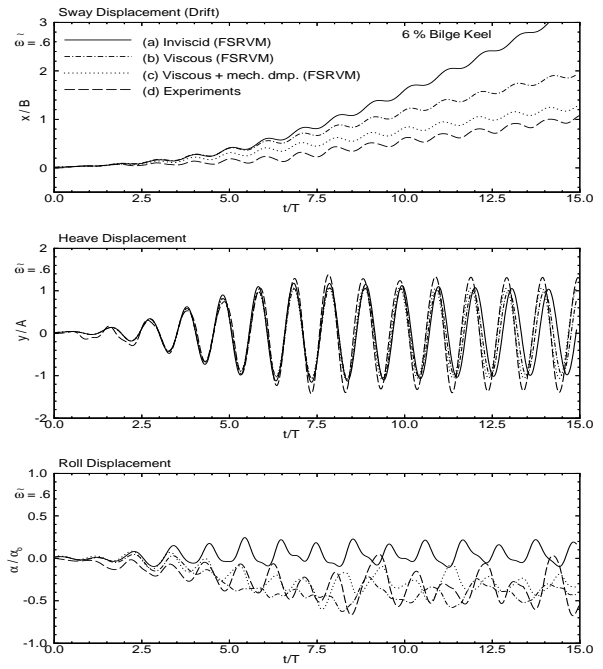


Figure 6: Motion response of freely-floating cylinder with 6% keels, $\tilde{\omega} = 0.6$

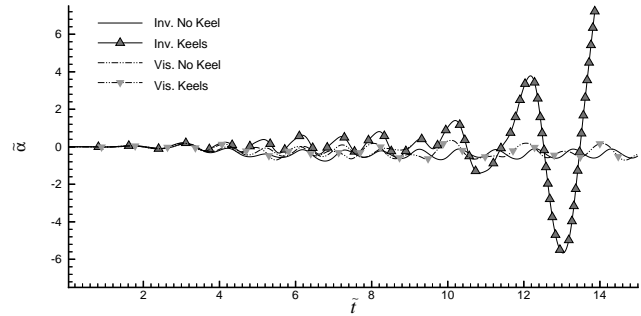


Figure 7: Numerical results of roll displacements for freely floating cylinders, $\tilde{\omega} = 0.746$

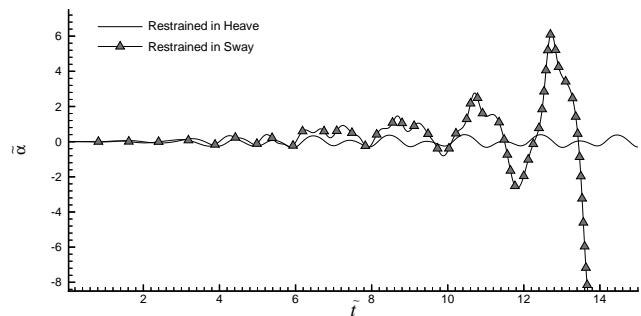


Figure 8: Inviscid results of roll displacements for restrained cylinder, $\tilde{\omega} = 0.746$